

## Two-fluid theory of thermal conductivity of dielectric crystals

Baxter H. Armstrong\*

*IBM Corporation, Palo Alto Scientific Center, 1530 Page Mill Road, Palo Alto, California 94304*

(Received 9 October 1979; revised manuscript received 26 August 1980)

A theory of lattice thermal conductivity is formulated in which phonons are divided into propagating and reservoir groups. At high temperatures, the groups are differentiated according to whether they occupy nondispersive modes below or dispersive modes above the U-process combination frequency threshold. Below this threshold, only N processes can be completed and it is assumed that there is no entropy production. Dissipation occurs in the rapidly relaxing reservoir modes above the threshold, and the heat current is carried by the more slowly relaxing phonons in the nondispersive modes. Appeal to the variational principle yields the result that the anharmonic relaxation rate for propagating modes is determined uniquely by the scattering into the reservoir modes. The theory carries over toward low temperatures with extrinsic resistivity providing reservoir relaxation in nondispersive modes as U processes die out. An explicit expression for the required anharmonic scattering rate for transitions to reservoir modes is adapted from existing acoustic absorption theory and combined with direct extrinsic scattering in the conventional way to provide the total relaxation time for the thermal conductivity. Minimum zone-boundary frequencies, maximum frequencies of nondispersive branches, a reservoir relaxation time, a Grüneisen gamma, and parameters for boundary and imperfection scattering are used as adjustable parameters to fit experimental thermal conductivities over broad temperature ranges for crystals of four major classes. Good to fair agreement is obtained for reasonable values of these parameters in all cases. Low-temperature relaxation times for N-process scattering into the extrinsic reservoir are in accord with conventional results except that they depend upon the purity of the specimen.

### I. INTRODUCTION

The calculation of heat conduction in nonmetallic crystals is, in general, a complex problem. Formulas advanced to span temperatures from the boundary scattering regime to the Debye temperature often require adjustable parameters that do not necessarily possess direct physical significance. Further, the formulas themselves are usually specific to a single-crystal class. Reviews of the theory have been given by Klemens,<sup>1,2</sup> Ziman,<sup>3</sup> and Carruthers,<sup>4</sup> and the books by Parrott and Stuckes<sup>5</sup> and by Berman<sup>6</sup> cover more recent developments. Slack<sup>7</sup> has prepared the most recent review, although he restricts his considerations to temperatures of the order of, or higher than, the Debye temperature. The present article addresses the applicability of acoustic absorption theory to the problem of thermal conductivity in the context of a division of thermal phonon modes into two groups. The absorption theory required can be drawn from the phonon-Boltzmann equation approach of Woodruff and Ehrenreich<sup>8</sup> or the Landau-Rumer theory as extended to account for finite thermal-phonon lifetimes by Simons and Maris.<sup>9</sup> Either approach can be used as a starting point since they turn out to be equivalent in the present domain of application, as discussed in Appendix A of Ref. 10.

The physical basis for the separation of modes into two categories, as described in Sec. II, arises from the difference between low-frequency

nondispersive modes dominated by anharmonic normal (N) processes, and higher-frequency modes dominated by thermally resistive processes. The low-frequency "propagating" modes carry the heat while the higher resistive modes provide dissipation that permits heat to leave the system. The resistive group is comprised towards high temperatures of those highly dispersive, low group velocity modes near the Brillouin-zone boundary (BZB) where umklapp- (U) process wave-vector reduction occurs. Towards low temperature, the resistive or "reservoir" group drops below the BZB plateau into the nondispersive part of the spectrum where frequency-dependent extrinsic resistive processes (isotope, impurity, dislocation scattering, etc.) become important as U processes die out. In this region, the distinction between the two groups becomes temperature dependent in a clearly defined manner, with the reservoir appearing in the high-frequency tail of the thermal-phonon distribution.

Viewed from the standpoint of scattering theory, the two-fluid theory is analogous to Mott's theory of electrical conductivity of transition metals.<sup>11</sup> The propagating phonons constitute a group with N-process interactions among its members that do not contribute to entropy production in the system. Thermal resistance appears through attenuation by scattering into the reservoir modes, by which process entropy production occurs in those modes. In the context of the phonon-Boltzmann-equation theory, the propagating phonons

constitute an assembly of classical waves that modulate the reservoir, causing it to depart from equilibrium.

Improvement is obtained relative to the Callaway approach<sup>4,6,12</sup> by identification of N processes that simply redistribute phonons among propagating modes, and for which the entropy production and contribution to the thermal current are negligible. When the remaining entropy production is maximized, the deviation from equilibrium of the distribution function for the propagating modes is determined uniquely in terms of the relaxation time for anharmonic transitions to reservoir modes. The physical interpretation of the two-fluid theory clarifies the nature of the N- and U-process relaxation times that influence thermal resistance. These ideas will be formalized in the next section with the choice of transition rates and definition of propagation and reservoir phonon groups or "fluids."

In Sec. III, boundary, imperfection, and impurity scatterings are incorporated with the anharmonic effect into a computational formula for the thermal conductivity  $K$ . Comparison of theory and experiment is carried out in Sec. IV for crystals of four major classes with agreement comparable to or better than prior theory. Special attention is given to LiF because of the wealth of studies available which have quantified the isotope scattering contribution to its thermal resistivity. High-temperature forms of the two-fluid expression for  $K$  are given in Appendix A. One of these is the conventional  $T^{-1}$  limit; the other is a very high-temperature limit of the form previously obtained by Slack.<sup>7</sup> Finally, Appendix B contains a discussion of the explicit relaxation-time forms that arise from the two-fluid theory as contrasted to conventional results. In Ref. 10, from which the present article is condensed, additional comparisons are given for Ge, SiO<sub>2</sub>, and ZnSO<sub>4</sub>, which extend the results to five crystal classes.

## II. TWO-FLUID ANHARMONIC RELAXATION MODEL

### A. Propagating and reservoir phonons in an ideal crystal

N processes, as is well known, should not contribute directly to thermal resistance because they conserve both energy and wave vector. However, an explicit fundamental expression of this behavior has not heretofore been available. In an ideal solid (viz., one in which only anharmonic interactions occur), U processes provide the necessary mechanism to dissipate momentum and create thermal resistance. This dissipation occurs only in modes that satisfy a certain threshold requirement. For a combination process  $\vec{q} + \vec{q}' \rightarrow \vec{q}''$ , where  $\vec{q}$  represents phonon wave vector,  $\vec{q}''$  must exceed one-half of a reciprocal-lattice vector. For decays  $\vec{q} \rightarrow \vec{q}' + \vec{q}''$ , the initial phonon must have a frequency above the lowest available BZB frequency. In both instances, the reduction of wave vector by the amount of a reciprocal-lattice vector occurs in modes that lie near or above the lowest BZB frequency. Separation of modes into those wherein only N processes can be completed, and those wherein U processes can be completed as well, permits a fundamental expression of the restriction on the contribution of N processes to thermal current. Because entropy production is proportional to thermal current, the requirement of no entropy production in modes below the U-process wave-vector reduction threshold is equivalent to the requirement that the thermal current exchanged among these modes vanishes. Thus the net thermal current associated with modes below this threshold arises from transitions to modes lying above the threshold. The fact that these two sets of modes usually have dramatically different characteristics leads to the utility of the proposed model for the computation of the anharmonic relaxation length.

Consider the total scattering rate for anharmonic processes,<sup>3</sup>

$$\left. \frac{\partial N_q}{\partial t} \right|_{AN} = \sum_{q'q''} \{ A(qq'q'') [N_q N_{q'} (N_{q''} + 1) - (N_q + 1)(N_{q'} + 1) N_{q''}] + B(qq'q'') [N_q (N_{q'} + 1)(N_{q''} + 1) - N_{q'} N_{q''} (N_q + 1)] \}, \quad (1)$$

where  $N_q$  is the occupation number of the mode with wave vector  $\vec{q}$ , and  $A(qq'q'')$  and  $B(qq'q'')$  reflect the transition rates for phonon combination and decay processes, respectively. Equation (1) can be split into two terms,

$$\left. \frac{\partial N_q}{\partial t} \right|_{AN} = \left. \frac{\partial N_q}{\partial t} \right|_{ANN} + \left. \frac{\partial N_q}{\partial t} \right|_{ANR}, \quad (2)$$

where  $(\partial N_q / \partial t)_{ANN}$  is the sum over modes  $\vec{q}'$  and

$\vec{q}''$  in which only normal processes can be completed (called "region 1"), and  $(\partial N_q / \partial t)_{ANR}$  is the remainder of the sum, taken over modes  $\vec{q}'$  and  $\vec{q}''$  in which U processes can be completed as well (called "region 2"). The threshold for region 2 can be identified approximately from experimental dispersion curve data showing BZB intersections. It should be noted that the second term of Eq. (2) includes both N- and U-process scattering con-

tributions. We employ the Boltzmann equation

$$\left. \frac{\partial N_q}{\partial t} \right|_{\text{AN}} = \vec{c}_q \cdot \vec{\nabla} T \frac{dN_q^0}{dT} \quad (3)$$

in the linearized approximation where  $\vec{c}_q$  is the group velocity of phonons in mode  $\vec{q}$ . The small deviation function  $\Phi_q$  is defined as

$$\Phi_q \equiv - (N_q - N_q^0) / \frac{\partial N_q^0}{\partial (\hbar\omega_q)} \quad (4)$$

(Eq. 7.71 of Ref. 3).  $N_q^0 \equiv N^0(\omega)$  is the occupation number  $[\exp(x) - 1]^{-1}$  of the equilibrium Bose distribution where  $x \equiv \hbar\omega / (k_B T)$ , and these latter symbols have their usual significance of the reduced Planck constant, angular frequency, Boltzmann constant, and absolute temperature, respectively. In the presence of a temperature gradient,  $\Phi_q$  can be expressed in terms of  $\tau(q)$ , a "total" relaxation time,<sup>1,12</sup> according to

$$\Phi_q = - \hbar\omega_q \tau(q) \vec{c}_q \cdot \vec{\nabla} T / T. \quad (5)$$

We now write the Boltzmann equation using the separation of Eq. (2), multiply it on both sides by  $(-\Phi_q/T)$ , and sum over all modes of region 1:

$$- \sum_{q(1)} \left. \frac{\partial N_q}{\partial t} \right|_{\text{ANN}} \frac{\Phi_q}{T} - \sum_{q(1)} \left. \frac{\partial N_q}{\partial t} \right|_{\text{ANR}} \frac{\Phi_q}{T} = \left( \sum_{q(1)} \hbar\omega_q c_q^2 \cos^2 \theta_q \tau(q) \frac{dN_q^0}{dT} \right) \left( \frac{\vec{\nabla} T}{T} \right)^2. \quad (6)$$

The sum on the right-hand side (rhs) has been re-expressed in terms of  $\tau(q)$ , and  $\theta_q$  is the angle between  $\vec{c}_q$  and  $\vec{\nabla} T$ . We now recognize the two terms on the left-hand side (lhs) of Eq. (6) as  $\dot{S}_{\text{NN}}$  and  $\dot{S}_{\text{NR}}$ , respectively, the rates of entropy production per unit volume due to scattering wholly within region 1 (NN), and from region 1 to region 2 (NR) (cf. Eq. 7.8.5 of Ref. 3). The prefactor on the rhs of Eq. (6) is the thermal conductivity  $K_1$  of the region-1 modes as given by Klemens (Eq. 46 of Ref. 2) so that the entire term is the total entropy-production rate in region-1 modes. We now assert, as the basis for the proposed two-fluid model, that the net entropy production due to NN scatterings vanishes. This property is expected of isolated N processes, but normally attributed to them only when a displaced Planck distribution exists [viz., a distribution such that  $\tau(q)$  in Eq. (5) is independent of  $q$ ]. In the presence of this special distribution, the entropy production of N processes vanishes for each scattering. We address here a more general situation where the entropy rate does not vanish for each individual scattering, but instead cancels in the mode sum. We write Eq. (6) as

$$(\dot{S}_{\text{NN}} + \dot{S}_{\text{NR}}) \cdot \vec{\nabla} T = \vec{J}_1 \cdot \vec{\nabla} T, \quad (7)$$

where  $\vec{J}_1$  is the total thermal current carried by region-1 modes,  $\vec{J}_{\text{NN}}$  the portion due to phonon flow via scatterings into other region-1 modes, and  $\vec{J}_{\text{NR}}$  is that due to flow via scatterings into region-2 modes. The above hypothesis sets  $\vec{J}_{\text{NN}} = 0$ , which produces the result

$$\vec{J}_1 = \vec{J}_{\text{NR}}. \quad (8)$$

Expressing  $(\partial N_q / \partial t)_{\text{ANR}}$  in the relaxation-time approximation

$$\left. \frac{\partial N_q}{\partial t} \right|_{\text{ANR}} = - \frac{\delta N_q}{\tau_{\text{ANR}}(q)}, \quad (9)$$

where  $\delta N_q \equiv N_q - N_q^0$ , Eq. (6) now yields

$$\sum_{q(1)} \delta N_q \hbar\omega_q \left( \frac{\tau(q)}{\tau_{\text{ANR}}(q)} \right) \vec{c}_q \cdot \frac{\vec{\nabla} T}{T} = \vec{J}_1 \cdot \vec{\nabla} T. \quad (10)$$

Comparison of this result with the basic expression for  $\vec{J}_1$ ,

$$\vec{J}_1 = \sum_{q(1)} \delta N_q \hbar\omega_q \vec{c}_q, \quad (11)$$

indicates that  $\tau(q) = \tau_{\text{ANR}}(q)$  is a solution to Eqs. (6) and (10) obeying Eq. (8). It is not unique, however, because any other  $\tau(q)$  of the form  $\tau(q) = \tau_{\text{ANR}}(q) + \Delta\tau_q$  is also a solution as long as  $\Delta\tau_q$  satisfies the relation

$$\sum_{q(1)} \delta N_q \hbar\omega_q \left( \frac{\Delta\tau_q}{\tau_{\text{ANR}}(q)} \right) \vec{c}_q \cdot \frac{\vec{\nabla} T}{T} = 0. \quad (12)$$

This nonuniqueness in  $\tau$  is due to the possibility that NN scattering, whose contribution vanishes in the mode sum, might affect the distribution by rearrangement of phonons among the modes. However, any such rearrangement leading to  $\Delta\tau_q \neq 0$  will *decrease* entropy production and therefore cannot be admitted. Substituting  $\delta N_q = - \vec{c}_q \cdot \vec{\nabla} T \tau(q) dN_q^0/dT$  into Eq. (12) we obtain

$$\dot{S}(\Delta\tau) = - \left( \frac{\vec{\nabla} T}{T} \right)^2 \sum_{q(1)} c_q^2 \cos^2 \theta_q \frac{(\Delta\tau_q)^2}{\tau_{\text{ANR}}(q)} C(q), \quad (13)$$

where  $C(q) \equiv \hbar\omega_q dN_q^0/dT$  and  $\dot{S}(\Delta\tau)$  is the entropy production due to the deviation  $\Delta\tau_q$ , which is seen to be inherently negative. The general variational principle of the linearized Boltzmann equation<sup>3,13</sup> can therefore be invoked to require  $\Delta\tau_q = 0$  to maximize the entropy production due to the ANR scattering that remains after  $\dot{S}_{\text{NN}}$  has been set to zero. This condition removes the nonuniqueness of  $\tau(q)$  and establishes that the departure from equilibrium of modal populations in region 1 is limited only by the NR scatterings. Thus we arrive at the result

$$\vec{J}_1 = \vec{J}_{\text{NR}} = - \left( \sum_{q(1)} c_q^2 \cos^2 \theta_q \tau_{\text{ANR}}(q) C(q) \right) \vec{\nabla} T \quad (14)$$

with  $\vec{J}_{\text{NR}}$  now independent of transition rates

among the NN modes, and the factor in large parentheses is again  $K_1$ . The above considerations are represented in Fig. 1, drawn to indicate that no heat current can escape region 1 (the propagation region) due to anharmonic processes (the role of extrinsic resistive processes as depicted in the figure will be discussed presently). The excitation within this region must escalate to modes within region 2 (the reservoir region) to exit the specimen.

Because of its importance to the above arguments, we now examine the single-mode relaxation-time approximation of Eq. (9). The scattering rate  $(\partial N_q/\partial t)_{\text{ANR}}$  for a region-1 mode can be expressed as<sup>3</sup>

$$\left. \frac{\partial N_q}{\partial t} \right|_{\text{ANR}} = - \frac{\delta N_q}{\tau_{\text{ANR}}(q)} - \int \int_{q(2)} (\Phi_{q'} - \Phi_{q''}) P_q^{q'q''} d^3q' d^3q'', \quad (15)$$

where  $P_q^{q'q''}$  are transition rates as defined by Ziman, with the integral taken over all  $\vec{q}'$  and  $\vec{q}''$  in region 2. This shows that the validity of Eq. (9) hinges upon the relative magnitudes of  $\Phi_{q'}$  and  $\Phi_{q''}$  over region 2 compared to  $\Phi_q$ . Our two-fluid model is predicated on the expectation that there exist reservoir modes nearly in equilibrium compared to the propagation modes such that<sup>14</sup>  $\Phi_{q'}, \Phi_{q''} \ll \Phi_q$  and  $\Lambda_{q'}, \Lambda_{q''} \ll \Lambda_q$ , where  $\Lambda_q$  is the relaxation length for mode  $q$ . These conditions are satisfied if

$$\frac{\Phi(\hat{q}_R)}{\Phi(\hat{q}_P)} = \frac{\hat{c}_R \hat{\omega}_R \tau(\hat{q}_R)}{\hat{c}_P \hat{\omega}_P \tau_{\text{ANR}}(\hat{q}_P)} \ll 1, \quad (16)$$

where R and P refer to reservoir and propagation groups and the caret signifies any mode in the group. There is generally a large group of modes with low to zero group velocity near the BZB which we assume will constitute reservoir modes satisfying Eq. (16). Furthermore, the thermal conductivity is proportional to  $\Lambda_q$  so we propose that this same characteristic permits the direct contribution of such modes to  $K$  to be neglected. Thus propagating phonons carry the heat in the two-

fluid model. We see from the above discussion that this model closely parallels the problem of absorption of a monochromatic acoustic wave by an assembly of thermal phonons. The approach proposed herein was, in fact, stimulated by the formulation of the Woodruff-Ehrenreich (WE) theory,<sup>8</sup> based on the indirect approach of Blount,<sup>15</sup> which already contains the idea of a reservoir that provides for dissipation of propagating phonons undergoing anharmonic scattering.

#### B. Anharmonic relaxation rate for propagating phonons

The relaxation length of a single mode is the absorption length for a sound wave of the same frequency, given by Landau-Rumer (LR) or phonon-Boltzmann equation theory.<sup>8-10,16</sup> For combination processes  $\vec{q} + \vec{q}' \rightarrow \vec{q}''$  with restriction of  $\vec{q}'$  and  $\vec{q}''$  to lie within the prescribed reservoir, this theory yields the absorption length  $\Lambda_{\omega j}$  for N-process transitions into the reservoir, according to<sup>10</sup>

$$\Lambda_{\omega j} = \frac{2\rho c_j^3}{\gamma_j^2 T \Delta C_R^{(j)} \omega \tan^{-1}(2\omega\bar{\tau})}. \quad (17)$$

The density is designated  $\rho$ ,  $c_j$  is an average sound speed for modes of polarization  $j$ ,  $\Delta C_R^{(j)}$  is the specific heat per unit volume of the selected reservoir modes with average relaxation time  $\bar{\tau}$ , and  $\omega$  is the frequency of the incident propagating phonon. The Grüneisen constant  $\gamma_j^2$  is defined relative to the sum of the two polarization terms of the acoustic theory.<sup>10</sup> For example, in an approximation of partial equality of longitudinal and transverse sound speeds,  $\gamma_T^2$  is given by

$$\gamma_T^2 \equiv [(c_T/c_L)\gamma_s^2(TL, L)\Delta C_L^{(j)} + 2\gamma_s^2(TT, T)\Delta C_T^{(j)}] (\Delta C_R^{(j)})^{-1}, \quad (18)$$

where the Grüneisen constant  $\gamma_s$  is defined by Maris,<sup>9</sup> and  $\Delta C_L^{(j)}$  and  $\Delta C_T^{(j)}$  are individual specific heats of the longitudinal and transverse phonons in the reservoir group. Strictly speaking,  $\bar{\tau}$ , along

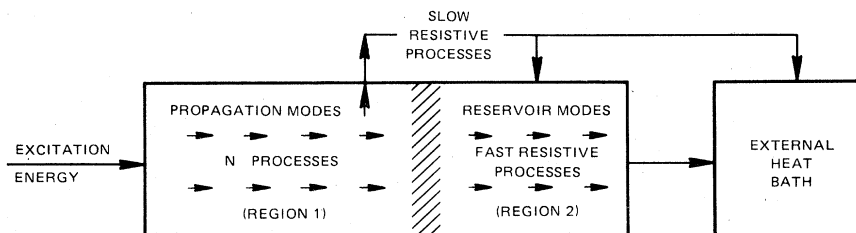


FIG. 1. Energy flow in the two-fluid model.

with the Grüneisen gamma, should be included in the specific-heat-weighted modal sum. However, neither is usually known well enough to warrant such an accurate treatment, so they are considered to be reservoir averages herein; in the same spirit we make the assumption of crystal isotropy throughout. Although the derivations that yield Eq. (17) do not include U processes, by definition of the reservoir the N-process transitions involved span the same modes  $\vec{q}'$  and  $\vec{q}''$  for which U processes are permitted. Therefore we assume U processes can be included by appropriate adjustment of the Grüneisen constant  $\gamma_m^2$ . Use of Eq. (17) implies neglect of the contribution of optic modes to the propagation group; we include them only in the reservoir. Nondispersive optic and other high-frequency modes with significant group velocity and relaxation times may contribute to thermal conduction. Since we formally omit them from the polarization sum for propagating modes, their presence will result in the inference of an excessive value for the Grüneisen gamma from the fit to experimental data (since this parameter normalizes the overall magnitude of  $K$ ). We obtain the ANR transition rate from Eq. (17) in a mean phonon approximation as

$$\tau_{\text{ANR}}^{-1}(\omega) = \frac{\gamma_m^2 T \omega \tan^{-1}(2\omega\tau)}{2\rho c_m^2} \left( \sum_j \int_{\omega_R}^{\omega_{RC}} C_{\omega_j}^{(v)} d\omega \right). \quad (19)$$

The Debye mean sound speed, obtained from the usual average of  $c_q^{-3}$  over all directions and polarizations, is denoted  $c_m$ ,  $\omega_R$  is the reservoir threshold angular frequency,  $\omega_{RC}$  is the frequency at which the reservoir spectrum is cut off, and  $\gamma_m$  is a mean Grüneisen constant.  $C_{\omega_j}^{(v)}$  is given by<sup>3</sup>

$$C_{\omega_j}^{(v)} = \frac{\mathfrak{N} k_B x^2 \exp(x) D_j(\omega)}{[\exp(x) - 1]^2}, \quad (20)$$

where  $D_j(\omega)$  is the fractional density of states of polarization  $j$ , and  $\mathfrak{N}$  is the number of unit cells per unit volume.

### C. Low-temperature reservoir due to extrinsic resistivity

The above considerations apply to an ideal crystal with only anharmonic interactions. Towards low  $T$ , extrinsic scattering such as that due to isotopes, impurities, dislocations, and crystal boundaries becomes more important than U processes in real crystals as a source of thermal resistance. For this reason, we now consider such extrinsic effects with regard to the distinction between propagation and reservoir modes, beginning with the specific case of the Rayleigh

scattering (RS) transition rate  $\tau_{\text{RS}}^{-1}(\omega)$  for impurity and/or isotope scattering,<sup>4, 17, 18</sup>

$$\tau_{\text{RS}}^{-1}(\omega) = \alpha (\bar{n}/k_B)^4 \omega^4. \quad (21)$$

For isotope scattering,  $\alpha$  is given by

$$\alpha \equiv V_0 \left( \sum_i f_i (1 - M_i/\bar{M})^2 \right) \left( \frac{k}{\bar{n}} \right)^4 / (4\pi c_m^3), \quad (22)$$

where  $V_0$  is volume per atom,  $f_i$  is the fraction of unit cells of mass  $M_i$ , and  $\bar{M}$  is the average unit-cell mass.

Although in real crystals no modes will be totally free of resistive loss, we suppose that a propagation region can still be defined if extrinsic resistive scattering is negligible compared to anharmonic resistive scattering. Thus for the propagation region we require, on the average,<sup>19</sup>

$$\tau_{\text{ANR}}^{-1}(\hat{\omega}_P) \gg \tau_{\text{RS}}^{-1}(\hat{\omega}_P). \quad (23)$$

By contrast, for the reservoir region we must require

$$\tau_{\text{RS}}^{-1}(\hat{\omega}_R) \gg \tau_{\text{ANR}}^{-1}(\hat{\omega}_P) \quad (24)$$

for this region to be in thermal equilibrium relative to the propagation region.  $\hat{\omega}_R$  and  $\hat{\omega}_P$  represent frequencies anywhere in the reservoir and propagation regions as in Eq. (16). There is now no threshold for onset of dissipative loss, and these strong inequalities cannot be satisfied over all of each region. However, a natural procedure is to separate the regions at the boundary of equality between the two scattering rates:

$$\tau_{\text{ANR}}^{-1}(\omega_R) = \tau_{\text{RS}}^{-1}(\omega_R) \quad (25)$$

such that  $\omega \leq \omega_R$  implies region 1 and  $\omega \geq \omega_R$  implies region 2.  $\omega_R$  now refers specifically to the frequency at the boundary between the two regions that is a solution to Eq. (25). With this definition, Eqs. (23) and (24) are satisfied only as weak inequalities ( $\geq$  and  $\leq$ , respectively). However, in the case of RS, the strong inequalities (23) and (24) become valid a short distance away from the boundary established by Eq. (25) because of the strong variation of  $\tau_{\text{RS}}^{-1}(\omega)$  with frequency compared to  $\tau_{\text{ANR}}^{-1}(\omega)$ . Therefore we still expect strong inequalities to hold true on the average and consequently the boundary defined by Eq. (25) to behave as a threshold. In view of the relative behavior of the two transition rates, we will also have  $\hat{\omega}_R \tau_{\text{RS}}(\hat{\omega}_R) < \hat{\omega}_P \tau(\hat{\omega}_P)$ , with the inequality becoming strong again a short distance from the boundary. This enhances the validity of the single-mode relaxation-time approximation [cf. Eq. (16)]. It is also true that  $\tau_{\text{ANR}}^{-1}(\omega)$  will no longer include a U-process contribution when transitions are completed in the extrinsic reservoir region below the wave-vector reduction threshold. We neglect this

effect in view of the lack of quantitative knowledge of anharmonic transition rates. The present considerations define the anharmonic scattering rate in a given propagation mode; when we compute the thermal conductivity, it will still be necessary to account for the direct resistive (e.g., Rayleigh) scattering out of the mode. The above inequalities also ensure that this latter rate is a small contribution to the direct scattering in region 1. This is illustrated in Fig. 1 by the arrows labeled "slow resistive processes" that connect propagation modes directly to the external heat bath. (Combined point-defect and anharmonic scattering as considered by Carruthers<sup>20</sup> may also connect propagation and reservoir modes as illustrated in the figure.)

The specific heat of the low-temperature reservoir arises from nondispersive acoustic modes because zone-boundary and optic modes will be unoccupied. Therefore the Debye approximation provides  $\Delta C_R^{(\omega)}$  as needed for a solution to Eq. (25) (Refs. 3 and 21):

$$\Delta C^{(\omega)} \simeq \left( \frac{9\bar{n}\rho R s}{w} \right) \left( \frac{T}{T_D} \right)^3 \int_{x_R}^{\infty} \frac{t^4 \exp(t) dt}{[\exp(t) - 1]^2}. \quad (26)$$

$R$  is the gas constant,  $\bar{n}$  the number of atoms per unit cell,  $s$  the number of primitive cells per molecule,  $w$  the molecular weight, and  $T_D$  the Debye temperature  $\hbar c_m (6\pi^2 \bar{n})^{1/3} / k_B$ . We expect<sup>10</sup> that  $\omega\tau \gg 1$  (although less than  $\omega\tau_p$ ), except at

very high  $T$ , so  $\tan^{-1}(2\omega\bar{\tau}) \approx \pi/2$ . Eq. (19) becomes

$$\tau_{\text{ANR}}^{-1}(x) \simeq QH(x_R)T^5 x, \quad (27)$$

where  $Q \equiv 9\pi\gamma_m^2 \bar{n} s R k_B / (4\hbar\omega c_m^2 T_D^3)$  and  $H(x)$  is

$$H(x) \equiv \int_x^{\infty} \frac{t^4 \exp(t) dt}{[\exp(t) - 1]^2}. \quad (28)$$

Use of Eqs. (21) and (27) in Eq. (25) yields

$$x_R^3 = QTH(x_R)/\alpha \quad (29)$$

from which the acoustic phonon frequencies to be included in the reservoir in the presence of Rayleigh scattering can be computed.

Equation (29) can be solved numerically or by use of a table of  $H(x)$  prepared from existing tabulations.<sup>22</sup> LiF forms a good illustration.<sup>17, 23</sup> We estimate  $\gamma_m$  by use of the thermal expansion value  $\gamma_{\text{th}} = 1.63$ .<sup>24</sup> Use<sup>25</sup> of  $\bar{n} = 2$ ,  $c_m = 4.96 \times 10^5$  cm/sec,  $T_D = 734$ , along with the remaining standard constants, yields  $Q = 0.16 \text{ sec}^{-1} \text{ deg}^{-5}$ . Curve  $B$  in Fig. 2 shows the reservoir boundary determined by Eq. (29) for this  $Q$  and  $\alpha = 0.03 \text{ sec}^{-1} \text{ K}^{-4}$  for specimen 2 of Ref. 17. Line  $A$  shows the U-process wave-vector reduction threshold (6.2 THz) obtained from the dispersion curves for LiF as the  $L_3$  (TA) normal-mode frequency (Table I and Fig. 4 of Ref. 26). Curve  $C$  will be discussed below. The values of  $x_R$  for curve  $B$  from 10 to 37 K range from 6.5 to 8, not substantially dif-

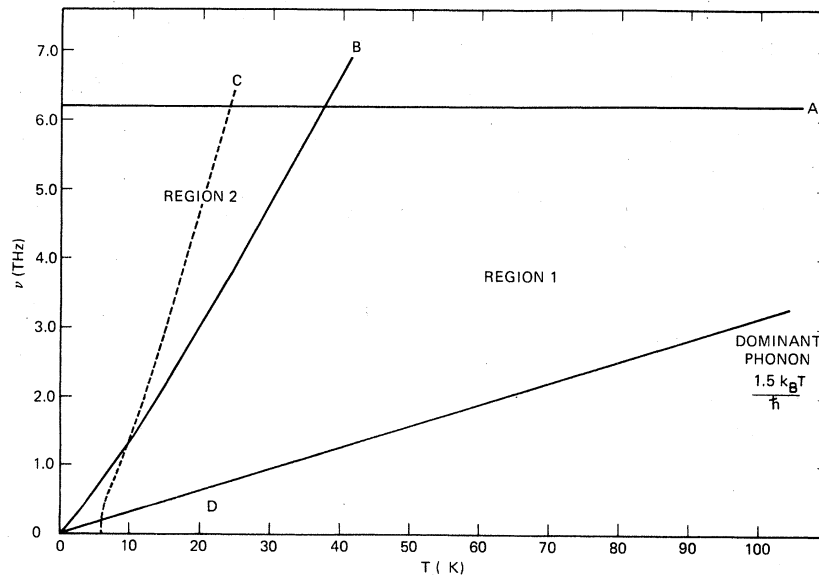


FIG. 2. Illustration of the two-fluid concept by a specific example. Region 1 is the normal-process dominated and region 2 the resistive-process-dominated region of the  $\nu$ - $T$  plane. Line  $A$  is the lowest zone-boundary intersection frequency where U processes begin. Curve  $B$  is the locus of points for which the anharmonic transition rate into modes above  $B$  equals the isotope scattering at that frequency. Curve  $C$  is the reservoir boundary for which dislocation and anharmonic scattering are equal for all frequencies. Line  $D$  represents the dominant phonon frequency.

ferent from a straight line. Line *D* is the "dominant phonon" frequency  $1.5k_B T/\hbar$ . The position of line *D* shows that for this relatively pure crystal the RS reservoir lies well into the thermal tail of the phonon distribution. Equation (27) is further discussed in Appendix B and shown to be similar to certain of the N-process relaxation rates inferred from Callaway analyses.<sup>27-32</sup> In addition, it leads indirectly to some of the U-process rates likewise inferred.<sup>17,23</sup>

It should be noted that the criteria established to separate propagation and reservoir regions are average as well as approximate conditions. Propagation modes of one polarization may extend above the U-process combination threshold of another polarization, and we expect to use some characteristic of the boundary between the regions as an adjustable parameter. Figure 3 illustrates the modes involved in the two roles on a dispersion curve diagram. The frequency of the BZB mode (usually highly dispersive) wherein the lowest U-process frequency combination can occur is designated  $\omega_{RU}$ . This is the reservoir threshold at high temperatures. The nondispersive portions of the TA and LA branches constitute the propagation modes so that  $\omega_p$  as shown in the figure is their (approximate) cutoff. Towards low temperatures, extrinsic resistive processes lower the reservoir into the nondispersive modes to the onset frequency  $\omega_R$ . Thus these modes may act in both propagation and reservoir roles as determined by the amount of extrinsic resistivity. Since at sufficiently low temperatures all occupied modes are nondispersive, these dual-role modes constitute the entire reservoir. For dislocation scattering we use the transition rate  $\tau_D^{-1}$  due to Klemens where

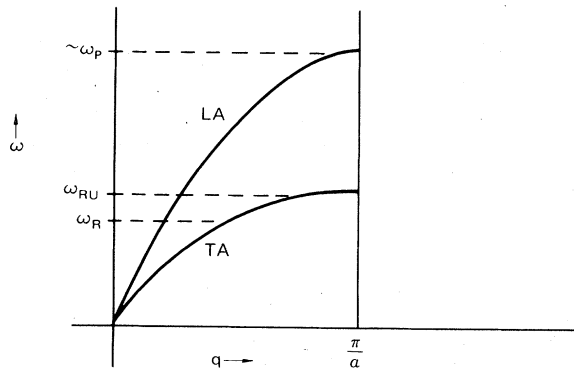


FIG. 3. Frequency limits for propagation and reservoir modes on an idealized phonon dispersion curve diagram. The U-process (high-temperature) reservoir threshold frequency is denoted  $\omega_{RU}$ , whereas the onset frequency of the low-temperature, nondispersive reservoir is  $\omega_R$ . A typical cutoff at the highest nondispersive propagating mode is designated  $\omega_p$ .

$\delta$  measures the scattering strength<sup>1</sup>:

$$\tau_D^{-1} = T\delta x. \quad (30)$$

This has the same frequency dependence as  $\tau_{ANR}^{-1}$ , so it will not create reservoir characteristics along the lines of our previous discussion. Nevertheless, it can limit the validity of the two-fluid model at low temperatures. The boundary for equality between  $\tau_D^{-1}$  and  $\tau_{ANR}^{-1}$  is

$$H(x_{RD}) = \delta/(QT^4). \quad (31)$$

Since this is independent of frequency, for reservoir boundary frequency above  $\omega_{RD}$ ,  $\tau_{ANR}^{-1}(\omega) < \tau_D^{-1}(\omega)$  for all  $\omega$ , and vice versa for boundary frequencies below  $\omega_{RD}$ . Curve C in Fig. 2 shows the critical frequency  $\omega_{RD}/(2\pi)$  as a function of  $T$  for  $\delta = 7500 \text{ sec}^{-1} \text{ K}^{-1}$  (specimen 2 of Ref. 17). Because  $H(x)$  has a maximum value  $H(0) = 25.98$ , below the minimum temperature  $T_M = (0.03849\delta/Q)^{1/4}$ , Eq. (31) cannot be satisfied and dislocation scattering dominates  $\tau_{ANR}^{-1}$  for all frequencies. Thus at sufficiently low  $T$ , dislocation scattering will cause the observed reservoir boundary to drop below  $\omega_R$  of Eq. (29) for RS, and the division into two groups of phonons loses significance near  $T_M$ . Fortunately,  $T_M$  appears in the ballistic regime (for reasonably pure crystals) where boundary scattering is becoming dominant and anharmonic processes are dying out. Therefore we neglect dislocation scattering in the determination of the reservoir.

Boundary scattering, insofar as it is independent of frequency, does not lead to reservoir behavior, so we neglect its effect on the determination of the reservoir. Like dislocation scattering, it will be included only in the direct resistive transition rate used to compute  $K$ .

### III. COMPUTATION OF THE THERMAL CONDUCTIVITY

#### A. Resultant mean phonon relaxation length

We now reduce the anharmonic thermal-conductivity expression implied by Eq. (14) to a mean phonon approximation. The fractional density of states  $D_j(\omega)$  [cf. Eq. (20)] in the approximation of a spherical surface in wave-vector space can be written<sup>21</sup>

$$D_j(\omega) = q_j^2/[2\pi^2 c_j(\omega)\mathfrak{V}]. \quad (32)$$

The group velocity  $c_j(\omega)$  in Eq. (32) cancels against the same factor in the expression for  $K$ , reducing the sensitivity of  $K$  to the effects of dispersion. The nondispersive approximation  $q_j = \omega/c_j$  is taken for the remaining factor  $q_j^2$  and a "mean phonon" relaxation length  $\bar{\Lambda}(\omega)$  is defined by

$$3\bar{\Lambda}(\omega)/c_m^2 \equiv \Lambda_{\omega L}/c_L^2 + 2\Lambda_{\omega T}/c_T^2, \quad (33)$$

where  $\Lambda_{\omega_L}$  and  $\Lambda_{\omega_T}$  are to be obtained from Eq. (17). Thus  $K$  becomes

$$K = \frac{k_B(k_B T/\hbar)^3}{2\pi^2 c_m^2} \int_0^{x'_D} \frac{x^4 \exp(x) \bar{\Lambda}(x) dx}{[\exp(x) - 1]^2}, \quad (34)$$

where  $x'_D = T'_D/T$ , and  $T'_D = (\hbar c_m/k)(6\pi^2 \mathcal{U})^{1/3}$  refers to acoustic modes alone.

To obtain a formula applicable to real crystals, it is assumed that in the propagation region, independent scattering mechanisms contribute by addition of reciprocal relaxation lengths. The resultant mean phonon relaxation length may then be expressed as

$$\bar{\Lambda}(\omega) = \bar{\Lambda}_b / [1 + \bar{\Lambda}_b/\bar{\Lambda}_{an}(\omega) + \bar{\Lambda}_b/\bar{\Lambda}_d(\omega) + \bar{\Lambda}_b/\bar{\Lambda}_{RS}(\omega)] \quad (35)$$

to account for boundary ( $b$ ), anharmonic ( $an$ ), dislocation ( $d$ ), and Rayleigh scattering ( $RS$ ), respectively. All terms of Eq. (35) are approximated as polarization averages and  $\bar{\Lambda}_b$  is taken as a simple frequency- and temperature-independent length. From Eqs. (30) and (21), we have

$$\bar{\Lambda}_d = \hbar c_m / (\hbar \omega \delta), \quad \bar{\Lambda}_{RS} = c_m / [\alpha (\hbar/k_B)^4 \omega^4]. \quad (36)$$

It is assumed that the parameters  $\bar{\Lambda}_b$ ,  $\delta$ , and  $\alpha$  can each be adjusted to account for the proper polarization and velocity averages. Application of the mean phonon definition of Eq. (33) to the anharmonic relaxation length of Eq. (17) implies that the mean Grüneisen constant  $\gamma_m$  of Eq. (19), which will also be taken as adjustable, is defined by

$$3c_m/\gamma_m^2 \equiv c_L/\gamma_L^2 + 2c_T/\gamma_T^2. \quad (37)$$

#### B. Reservoir specific heat and relaxation time

The density of states for dispersive reservoir modes was taken as a constant function of frequency from the U-process reservoir threshold  $\omega_{RU}$  to the end of the spectrum, designated  $\omega_{RC}$ . All optic modes were assigned to the reservoir, along with acoustic modes of small group velocity.

$$\Delta C_R^{(w)} = \frac{3R\rho s}{w} \left[ 3\bar{n} \left( \frac{T}{T_D} \right)^3 [J_4(x_{RU}) - J_4(x_R)] \Delta(x_R, x_{RU}) + \frac{\bar{n} - \frac{1}{3} - \frac{2}{3} (g/b)^3}{f^{-1} - b^{-1}} \left( \frac{T}{T_D} \right) [J_2(x_{RC}) - J_2(x_{RU})] \right], \quad (42)$$

where  $\Delta(x_R, x_{RU})$  is equal to 1 if  $x_R \leq x_{RU}$  and to 0 if  $x_R > x_{RU}$ . Although procedures for estimation of  $x_R$  were outlined in Sec. IIC above, for simplicity we take  $x_R$  to be a temperature-independent adjustable parameter. The error this introduces, as well as that of the discontinuous low-temperature reservoir onset used in Eq. (42), will be treated later.

A procedure to estimate  $\bar{\tau}$ , which is expected to

decrease uniformly with  $T$ ,<sup>33</sup> is available from the approximation that the reservoir phonon energy  $\hbar\hat{\omega}_R \gg k_B T$  so that reservoir relaxation is dominated by the decay of optic phonons into acoustic phonons of roughly equal frequencies. The theory for this process<sup>34,35</sup> suggests the use of

$$\tau(\hat{\omega}_R)^{-1} = \tau_0^{-1} [1 + 2N^0(\hat{\omega}_R/2)] \quad (43)$$

as the reservoir relaxation time, where  $\tau_0$ , which

$$\Delta C_f^{(w)} = \frac{3R\rho s(k_B T/\hbar)}{w(\omega_{RC} - \omega_{RU})} (f_A + \bar{n} - 1) [J_2(x_{RC}) - J_2(x_{RU})], \quad (38)$$

where  $J_2(x)$  is a member of the family of Debye integrals

$$J_n(x) \equiv \int_0^x \frac{t^n \exp(t) dt}{[\exp(t) - 1]^2}. \quad (39)$$

As noted in Sec. IIC, towards low temperature, extrinsic resistive processes begin to couple additional modes that lie below the U-process plateau into the reservoir. These modes begin at  $x_R \equiv \hbar\omega_R/k_B T$  as long as  $\omega_R \leq \omega_{RU}$ , and their specific heat is

$$\Delta C_D^{(w)} = \frac{9R\rho s}{w} \left( \frac{T}{T_D} \right)^3 [J_4(x_{RU}) - J_4(x_R)]. \quad (40)$$

Since this "Debye tail" of the reservoir involves only acoustic modes,  $T'_D$  has been used in place of  $T_D$ . However, it was found computationally convenient to reduce all frequencies to the scale of the conventional Debye frequency by means of the dimensionless numbers  $b$ ,  $f$ , and  $g$  defined as

$$b \equiv \omega_D/\omega_{RU}, \quad f \equiv \omega_D/\omega_{RC}, \quad g \equiv \omega_D/\omega_P. \quad (41)$$

With these definitions, the total reservoir specific heat becomes

will be used as an adjustable parameter, is independent of  $T$ . We now replace  $\hat{\omega}_R$  by  $\frac{1}{2}\omega_D$  as a crude average to obtain an interpolation formula for  $\bar{\tau}$ . Phonon-linewidth information provides an experimental estimate of  $\tau(\hat{\omega}_R)$  as  $(\Delta\hat{\omega}_R)^{-1}$  where  $\Delta\hat{\omega}_R$  is the width of the dispersion curve.<sup>36</sup> The corresponding value of  $\tau_0$  in units of  $\omega_D^{-1}$  is given by Eq. (43) as

$$A_0 \equiv \omega_D \tau_0 = \frac{\omega_D}{\Delta\hat{\omega}_R} \left( 1 + \frac{2}{\exp[T_D/(4T)] - 1} \right). \quad (44)$$

$$K = \frac{\bar{\Lambda}_b k_B^4 T^3}{2\pi^2 \hbar^3 c_m^2} \int_0^{x_P} \frac{x^4 \exp(x) dx}{[\exp(x) - 1]^2 [1 + B_{an} x \tan^{-1}(Ax) + B_d x + B_{RS} x^4]}. \quad (45)$$

The coefficients in this expression are defined by

$$\begin{aligned} B_{an} &\equiv [\bar{\Lambda}_b \gamma_m^2 T^2 \Delta C_R^{(v)} (k_B/\hbar)] / (2\rho c_m^3), \\ B_d &\equiv \bar{\Lambda}_b T \delta / c_m \\ B_{RS} &= \bar{\Lambda}_b \alpha T^4 / c_m, \\ A &\equiv 2k_B T \bar{\tau} / \hbar = \frac{2A_0 T / T_D}{1 + 2 \{ \exp[T_D/(4T)] - 1 \}^{-1}}, \end{aligned} \quad (46)$$

where  $\Delta C_R^{(v)}$  is given by (42). We have replaced  $x_D$  by  $x_P$  in the upper limit of the integral in Eq. (45) since it will be adjusted to cut off the propagation modes in the presence of dispersion and contributing optic modes. Although suggested by the experimental dispersion relation curves,  $\omega_{RU}$  will also be adjusted in view of the neglect of the temperature dependence of the Grüneisen gamma, and polarization of the approximate final-state density, and to reflect the average effect of anisotropy (since  $\omega_{RU}$  is strongly dependent on the direction of phonon propagation). The cutoff  $\omega_{RC}$  was not varied; it was taken from experimental dispersion curves.

Equation (45) was numerically integrated with 48-order Gaussian quadrature.<sup>22</sup> The calculations, programmed in FORTRAN IV, were carried out interactively under the VM/370 CMS operating system on IBM Model 145 and 158 computers. The parameters were adjusted by subjectively changing input data to the program at the terminal until agreement was achieved between the computation and the experimental data for a given crystal.

#### IV. COMPARISON OF THEORY AND EXPERIMENT

##### A. General considerations

Although an isotropic approximation, Eq. (45) provided sensible agreement with experiment for all anisotropic as well as isotropic crystals investigated over appropriate temperature regions. Consequently, comparisons will be presented for cubic, hexagonal, tetragonal, and trigonal struc-

$A_0$ , as inferred from the fits to  $K$ , will be compared to the experimental linewidth, where available, by use of this relation. The rhs of Eq. (44) will be referred to as  $A_0(\text{exp})$ .

##### C. General computational formula

Equations (34)–(37) yield the final computational formula for  $K$ :

tures. Comparisons for orthorhombic  $\text{ZnSO}_4$ , for natural and isotopically enriched Ge, and for  $\text{SiO}_2$  are given in Ref. 10, along with further discussion of the cases considered here. The densities, Debye mean sound speeds, and Debye temperatures were obtained, with one exception, from the compilation of Anderson.<sup>25</sup> For  $^4\text{He}$ ,  $T_D$  and  $\rho$  were taken from Berman *et al.*<sup>37</sup> to match the specimen on which  $K(T)$  was measured, and  $c_m$  was estimated from the results of Crepeau *et al.*<sup>38</sup> These material properties for all crystals studied, along with the adjustable parameter values obtained from fitting the theoretical curves to the data, are collected in Table I. The letters (a), (b), etc., for certain crystals listed in the table refer to curves of the figure showing  $K(T)$  for different compositions or directions [curves (b), (c), and (d) for LiF are for specimens 2, 3, and 5, respectively, of Ref. 17].

Thermal-conductivity data for LiF and  $^4\text{He}$  were read from the graphs in Refs. 17 and 37, respectively. For the case LiF (a), datum points were kindly supplied by Dr. Philip D. Thacher.<sup>39</sup> For  $\text{Al}_2\text{O}_3$  and  $\text{TiO}_2$ , data were taken from the compilation of Touloukian *et al.*<sup>40</sup>

The RS strength  $\alpha$  was used as an adjustable parameter in spite of the availability of theoretical values as a test of the present theory and fitting procedure. Comparison of inferred and theoretical values was generally reassuring. The results, discussed in Ref. 10, ranged from essentially precise agreement for LiF (b) and  $\text{SiO}_2$  to a maximum 50% discrepancy for Ge and  $\text{TiO}_2$ . A comparison is also given there of inferred  $x_R$  values with "theoretical"  $x_R$  values as computed from Eq. (29) using inferred  $\alpha$  values. This comparison, although quite good in several cases, shows only qualitative agreement in others, which is attributed to the variation of  $T_D$  with  $T$ . The specification of  $T_D$  for the low-temperature reservoir may be particularly sensitive to this variation, especially since these reservoir modes span only

TABLE I. Input data (left-hand side) and inferred parameters (right-hand side) of the thermal conductivity curves of Figs. 4–8.  $c_m$  and  $T_D$  are the Debye sound speed in km/sec and temperature in K, respectively.  $f$ ,  $b$ , and  $g$  are dimensionless ratios of the Debye frequency to frequencies of, respectively, the spectrum limit, U-process reservoir threshold, and propagation mode cutoff.  $\gamma_m$  is a Grüneisen constant,  $\Lambda_b$  the boundary length in mm,  $\delta$  the dislocation strength in  $\text{sec}^{-1} \text{K}^{-1}$ ,  $A_0$  the reservoir relaxation time in reciprocal Debye frequency units,  $\alpha$  the Rayleigh scattering strength in  $\text{sec}^{-1} \text{K}^{-4}$ , and  $x_R \equiv \hbar \omega_R / k_B T$ , where  $\omega_R$  is the onset angular frequency of low-temperature reservoir modes.

Species	$c_m$	$T_D$	$f$	$\gamma_m$	$b$	$g$	$\Lambda_b$	$\delta$	$A_0$	$\alpha$	$x_R$
LiF (a)							9.6	200		0.0015	8.2
(b)							4.6	500		0.0019	8.0
(c)	4.963	734	0.77	1.45	2.8	1.4			1000		
(d)							4.6	1000		0.30	6.0
							4.6	4000		1.18	5.8
$^4\text{He}$ (a)				2.46	2.2		(7)	0	100		20–25
(b)	0.29	28.7	0.65	0.925	3.7	1.1	(4)	0	10		
$\text{Al}_2\text{O}_3$	7.026	1020	0.82	1.378	2.78	1.88	4.0	1500	100	0.0083	7.8
$\text{TiO}_2$	5.557	712	0.62	3.31	4.6	0.65	2.0	0	5	0.24	5.7

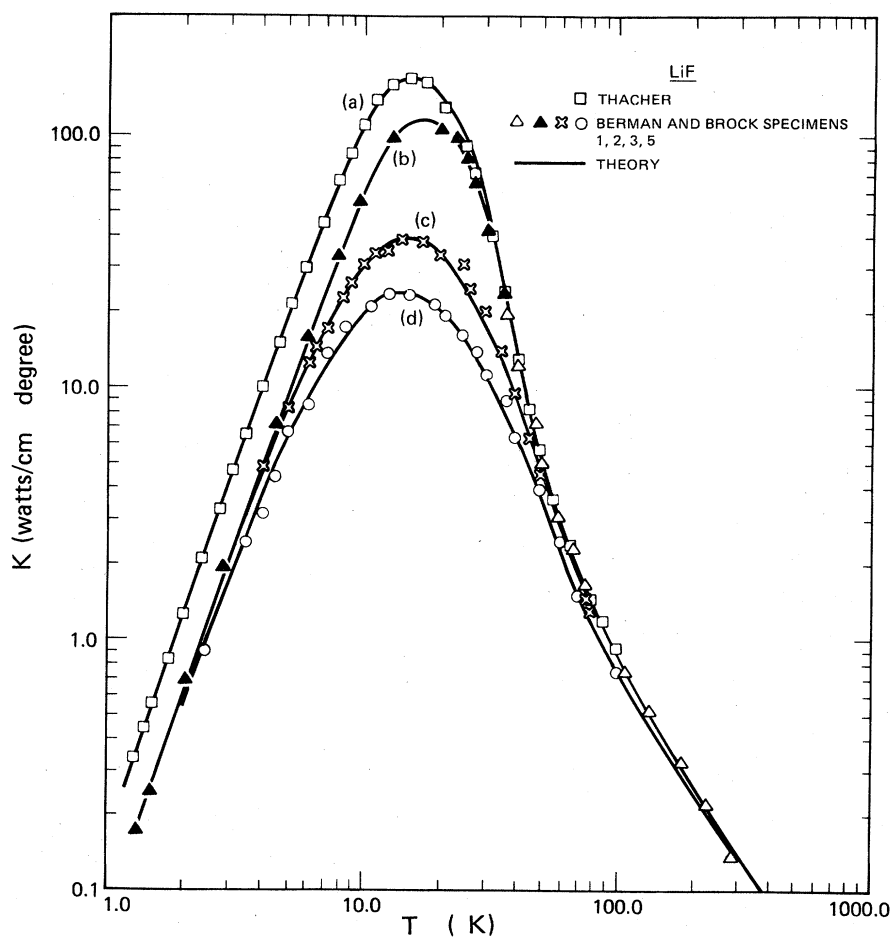


FIG. 4. Comparison of theory and experiment for LiF. The experimental points are from Thacher ( $\square$ ; Ref. 23) and from Berman and Brock ( $\Delta$ , specimen 1,  $\blacktriangle$  specimen 2,  $\times$  specimen 3,  $\circ$  specimen 5; Ref. 17). The theoretical curves correspond to different values of the scattering strength  $\alpha$  and other adjustable parameters as given in Table I of the text.

a high-frequency subset of the spectrum.

Since the reservoir relaxation parameter  $A_0$  enters through the arctangent function,  $K$  is not very sensitive to its magnitude unless  $A_0 < \sim 10$ . The computation is also somewhat insensitive to the precise value of the dislocation strength (a feature shared by prior analyses).

#### B. Cubic: LiF

Figure 4 for LiF shows the comparison between theory, Thacher's experimental measurements [curve (a),  $\square$ ; these data correspond to curve A of Figs. 1 and 4 of Ref. 23], and measurements of Berman and Brock<sup>17</sup> [curves (b),  $\Delta$ ; (c),  $\times$ ; (d),  $\circ$ ]. The  $b$  value of 2.8 required for the fit corresponds to a U-process reservoir threshold somewhat below the TA branch zone-boundary intersections (but not as low as was obtained in the Berman-Brock and Thacher-Calloway fits). The BZB intersections occur at  $b = 2.5$  in the [111] direction, and at  $b = 2.0$  in the [001] and [110] directions.<sup>26</sup> This lowering may be due to compensation for the constant Grüneisen gamma (the inferred  $\gamma_m$  was 1.45 compared to 1.63 for the thermal-expansion value) of the fit. The behavior of the conventional elastic-constant gammas as functions of  $T$  could produce a similar effect to that of increased  $b$  (as  $b$  increases, the peak value of  $K$  drops).

In cases (b) and (c), significantly lower values of  $\delta$  were required than those adopted by Berman and Brock. Our values are in the range 10–15 times smaller that would produce agreement with Klemen's predicted values according to the dis-

cussion of Berman and Brock. Such anomalously large  $\delta$  values characteristic of Callaway fits<sup>31</sup> may arise from the missing dependence of  $\tau_N^{-1}$  in that theory on isotopic composition. The propagation-mode cutoff frequency  $\nu_p = \nu_D/g = 11$  THz exhibits excellent consistency with the maximum LA frequency of  $\sim 12$  THz which begins to show significant dispersion above about 10 THz.

The four curves of Fig. 4 exhibit a significant discrepancy in the vicinity of the onset of the low- $T$  nondispersive contribution to the reservoir. Therefore, it is of interest to determine the error introduced by the straight-line approximation to the nondispersive reservoir boundary. Two further cases out of the measurements made by Thacher—the data shown on curves B and D of Fig. 4 of Ref. 23—were selected for a numerical experiment to infer the exact reservoir boundary on a point-by-point basis. First, an initial fit was made to the  $K$  data, as in Fig. 4 herein, to determine optimum adjustable parameter values. Then a second calculation was performed using these parameters as obtained from the fit *except for*  $\alpha$  and  $x_R$ . The theoretical values given by Thacher were used for  $\alpha$ , and the value of  $x_R$  was calculated that produced exact agreement between the experimental and theoretical values of  $K$  (to the three figures determined in Thacher's experiments). Use of nonzero  $\delta$  did not seem to improve the fits, so dislocation scattering was neglected. Figure 5 shows as open circles the results of this point-by-point inference of  $x_R(T)$  as plotted in the frequency-temperature plane for Thacher's case B, with  $\alpha$

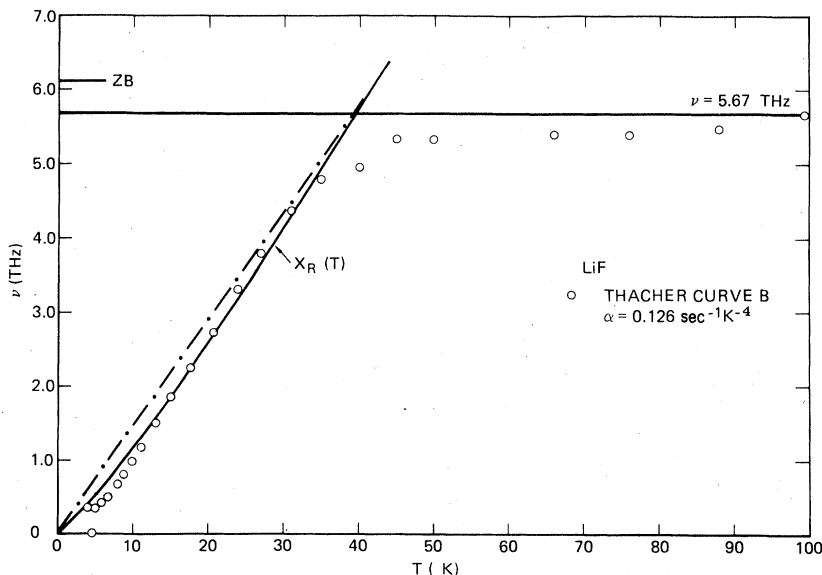


FIG. 5. Inference of "exact" reservoir boundary frequencies and comparison with theoretical boundaries (solid and broken curves) of the two-fluid model. The open circles are boundary frequencies for which the theoretical formula for  $K$  reproduces the experimental values as measured by Thacher (curve B of Ref. 23).

fixed at  $0.126 \text{ sec}^{-1} \text{ K}^{-4}$ . The lowest BZB frequency is marked on the figure as well as the inferred high-temperature reservoir frequency of 5.67 THz. The solid sloping curve gives  $x_R(T)$  computed from Eq. (29) for the value  $Q/\alpha = 1.86 \text{ K}^{-1}$  that most closely matches the experimental points. The dash-dot straight line beside the  $x_R(T)$  curve has the slope 6.9 selected in the initial fit. This selection was made before the second calculation was done so that the results of the latter did not influence the choice. Similar results were obtained for Thacher's case D.

In general, Fig. 5 confirms the reservoir concept formulated above. The high-temperature points (i.e., above the low-temperature reservoir onset  $\sim 40 \text{ K}$ ) slowly drift upward relative to a horizontal line—probably due mainly to temperature variations of the Grüneisen gamma and U-process combination threshold. This drift, plus the smooth transition region between the two reservoirs, is clearly responsible for most of the error in the fits, which are highly sensitive to the reservoir boundary.

Below about 12 K, the inferred boundary frequencies begin to increasingly drop below the theoretical RS curve. Variation of  $T_D$  with  $T$  may contribute to this effect along with dislocation scattering and a possible frequency-dependent component of the boundary scattering. An especially interesting feature of Fig. 5 is the persistence of a smooth, well-defined reservoir boundary below the thermal conductivity maximum, which is at 15 K for this crystal.<sup>23</sup> Thus the reservoir determination appears independent of the boundary scattering, which exceeds the anharmonic scattering in this temperature range. The last two points shown on the figure, at 4.6 and 4.0 K, have begun to fluctuate because the size of the anharmonic contribution has reached the error in the fit to the data. Therefore, it is not possible to confirm whether or not all modes become resistive in the reservoir sense before the reservoir loses significance.

#### C. Hexagonal: $^4\text{He}$

Figure 6 gives the comparison with experimental data taken from Berman *et al.*<sup>37</sup> for heat flow  $78^\circ$  to the  $c$  axis [ $\circ$ , curve (a)], and flow  $6^\circ$  to the  $c$  axis [ $\bullet$ , curve (b)]. The inferred  $b$  values are 2.2 and 3.7, respectively, while the observed U-process combination thresholds in the [1010] and [0001] directions are about 0.24 and 0.18 THz, respectively, corresponding to  $b$  values of 2.5 and 3.3,<sup>41,42</sup> (the Berman *et al.* crystal had molar volume  $20.2 \text{ cm}^3$ ). Thus, our U-process reservoir threshold for  $c$ -axis flow is below the lowest observed zone-boundary intersection as in the case

of LiF above. Our  $\gamma_m = 2.46$  for flow at  $78^\circ$  to the  $c$  axis is comparable to the thermal-expansion value. Berman *et al.* obtain  $b$  values of 2.53 and 4.64, corresponding to still lower thresholds than ours. Because of the inapplicability of our theory in the region of the maximum, due to the onset of Poiseuille flow, it was not possible to infer  $\alpha$  values below the temperature of the maximum and the boundary lengths used in the fit are enclosed in parentheses in Table I to indicate their unreliability.

Reese *et al.*<sup>42</sup> have measured linewidths for the LA and LO branches for the  $c$ -axis direction in  $^4\text{He}$  at  $16 \text{ cm}^3/\text{mole}$ . The frequency scaling with molar volume which they discuss indicates that the values of  $A_0(\text{exp}) = 3-5$  obtained from their measurements should also pertain to our case. The inferred value of  $A_0 = 10$  for nearly parallel flow provides reasonable agreement for this direc-

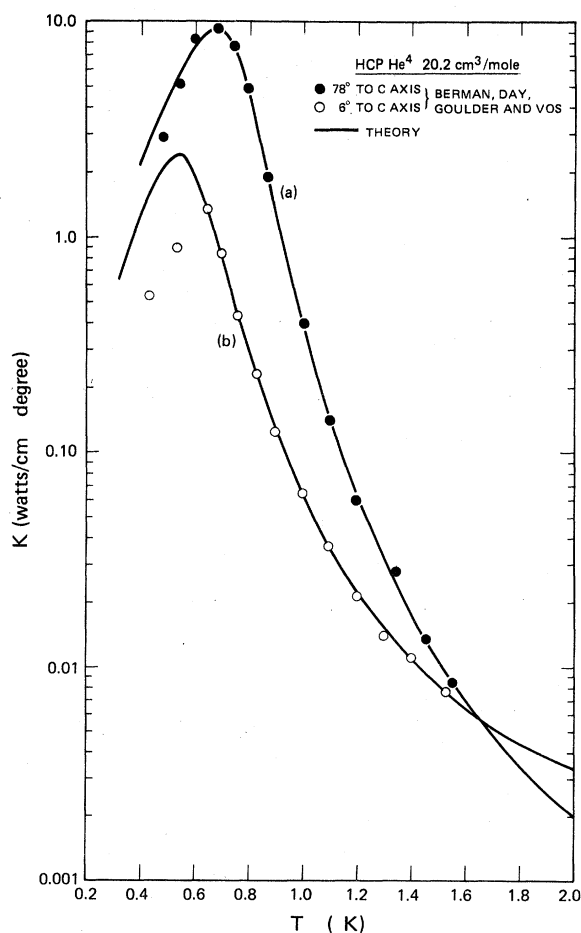


FIG. 6. Comparison of theory and experiment for hcp  $^4\text{He}$  with molar volume  $20.2 \text{ cm}^3$ . The experimental points from Berman, Day, Goulder, and Vos (Ref. 37) are for heat flow  $78^\circ$  to the  $c$  axis ( $\bullet$ ) and  $6^\circ$  to the  $c$  axis ( $\circ$ ).

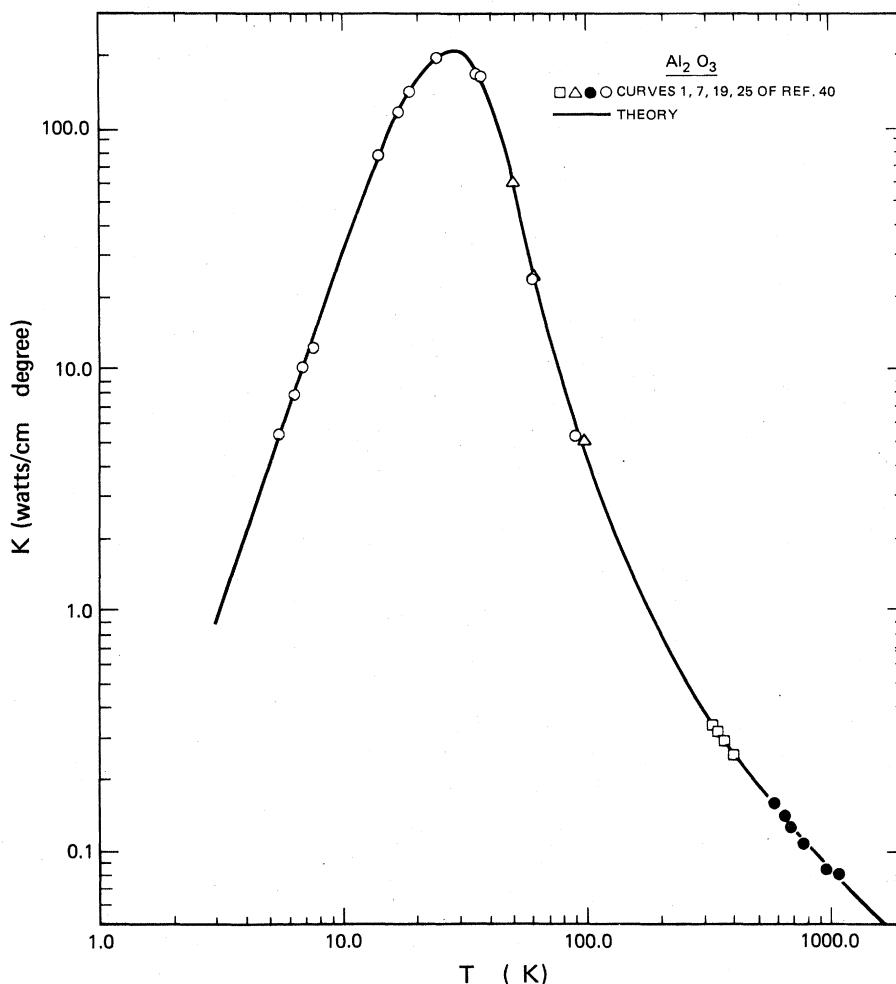


FIG. 7. Comparison of theory and experiment for sapphire. Data points marked  $\square$   $\Delta$   $\bullet$   $\circ$  are from curves 1, 7, 19, and 25, respectively, of Fig. 15 of Ref. 40. The theoretical curve parameters are given in Table I of the text.

tion. For the transverse directions they obtained only upper limits on the linewidths, which are considerably broader than the width implied by our inferred value  $A_0 = 100$ .

#### D. Trigonal: $\text{Al}_2\text{O}_3$

The fit of Fig. 7 for  $\text{Al}_2\text{O}_3$  is remarkably good, partly due, no doubt, to the broad expanses of temperature range without data. The data are due to ( $\square$ ) Koenig, ( $\bullet$ ) Kingery and Norton, ( $\Delta$ ) Berman, and ( $\circ$ ) Berman *et al.*, as referenced in Fig. 15 of Touloukian *et al.* for curves 1, 19, 7, and 25, respectively. The U-process reservoir threshold  $\nu_D/b = 7.65$  THz lies above the lowest zone-boundary TA frequencies at about 6 THz.<sup>43</sup> The LA branches appear to be more dispersive than the TA in this crystal. Our inferred propagation-mode cutoff of 11.3 THz agrees precisely with the BZB frequency of the highest nondispersive branch

which is TA.

The inferred  $\gamma = 1.378$  is close to the thermal-expansion gamma value 1.32. At the time the curve was drawn, the points  $\bullet$  from 600 to 1100 K, due to Kingery and Norton, had not been found by the author, so they did not influence the choice of parameters. It was, therefore, a pleasant surprise after discovering these data upon a closer examination of Ref. 40, to find that they fitted so well on the already drawn curve.

#### E. Tetragonal: $\text{TiO}_2$

The comparison for this crystal is given in Fig. 8, which includes data<sup>40</sup> due to Thurber and Mante ( $\circ$ ), Charvat and Kingery ( $\square$ ), Kingery and Norton ( $\nabla$ ), McCarthy and Ballard ( $\bullet$ ), and Berman, Foster, and Ziman ( $\Delta$ ). An interesting aspect is the unambiguous presence of nondispersive optic modes<sup>44</sup> which may be expected to contribute to the

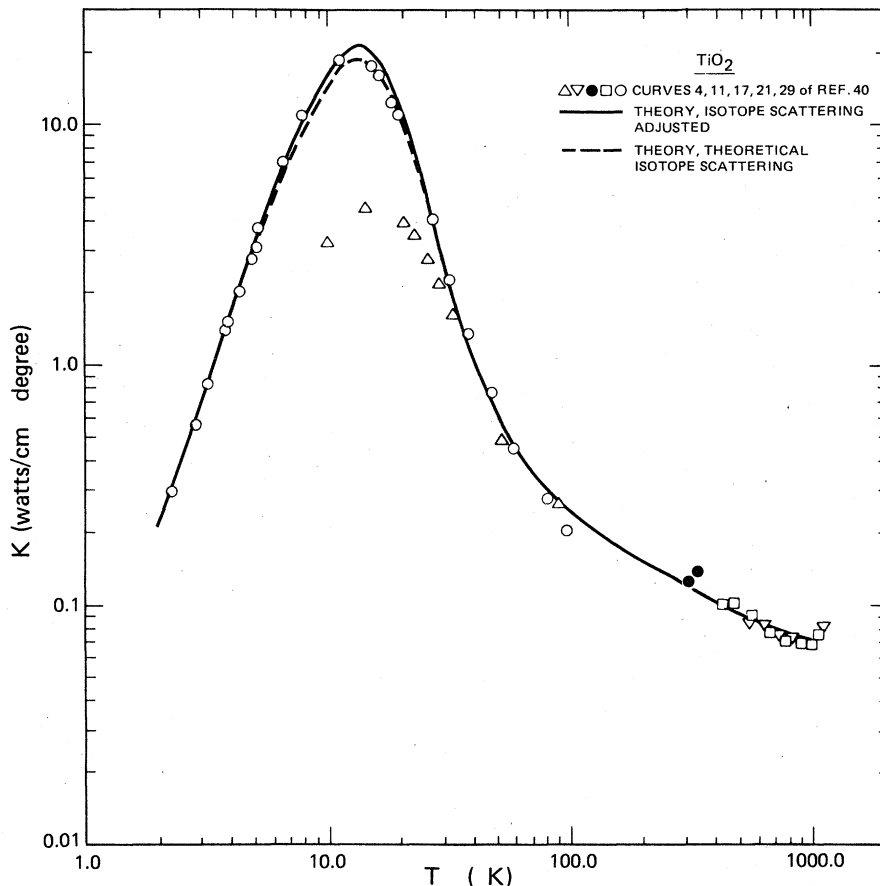


FIG. 8. Comparison of theory and experiment for rutile. The data points marked  $\Delta$   $\nabla$   $\bullet$   $\square$   $\circ$  are from curves 4, 11, 17, 21, and 29, respectively of Fig. 36 of Ref. 40. The parameters of the theoretical curve are given in Table I of the text.

propagation group. This is confirmed by the fit; the propagation-mode cutoff parameter  $g$  has the value 0.75, the smallest by far of the cases analyzed herein. Although this corresponds to 19.8 THz, almost 8 THz above the highest acoustic modes, it is consistent with the neutron scattering data. As in the case of  $\text{SiO}_2$  above, the inferred  $\gamma_m = 3.31$  is much larger than the thermal-expansion gamma 1.3, tending to support the optic-mode involvement in propagation. Our inferred U-process reservoir threshold at 3.2 THz ( $b = 4.6$ ) is just above the lowest zone-boundary modes<sup>44</sup> at 3 THz.

The dashed curve in Fig. 8 has been drawn for the theoretical value of  $\alpha = 0.46 \text{ sec}^{-1} \text{ K}^{-4}$  for isotope scattering. It provides a better fit on the high-temperature side of the maximum at the expense of some of the points in the boundary scattering regime.

#### V. CONCLUSION

The two-fluid theory presented herein has the

advantage of possessing a fundamental basis in the variational principle while at the same time exploiting dispersion and density-of-states complexities that commonly hinder the implementation of prior approaches. It also provides a more precise definition of the contribution of N processes to thermal resistance than previously available, and results in a more intimate connection between isotope and/or impurity scattering and anharmonic scattering than has been realized before. The combination of N- and U-process transition rates into a single anharmonic term conveniently reduces the number of potential adjustable parameters, and, while a large number is still employed in the approach as presented herein, reduction can be made by further refinements. The two-fluid theory appears to unify thermal-conductivity phenomena over a considerably broader temperature range than individual prior approaches, with a single set of parameters determining the conductivity from the boundary scattering regime to above the Debye temperature.

## ACKNOWLEDGMENTS

I would like to express my deep appreciation to Dr. Horace P. Flatt for continued support and encouragement during the lengthy evolution of this work, to the IBM Corporation for granting me a sabbatical year in which to pursue it, and to Professor Daniel Bershader for the opportunity to work on it at Stanford. Major credit and profound thanks are due to Ray Orbach, who patiently led me out of a wilderness of intuitive previous versions.

APPENDIX A: HIGH-TEMPERATURE ASYMPTOTIC FORMS OF  $K$ 

## 1. Intermediate high-temperature limit

At high temperatures, one can neglect all but the anharmonic processes. Using  $J_n(x) \approx x^{n-1}/(n-1)$ , and setting  $\mathfrak{F} \equiv [n - \frac{1}{3} - \frac{2}{3}(g/b)^3]$ ,  $K$  [Eq. (45), text] becomes

$$K = \frac{(k_B/\hbar)^2 M c_m T}{3\pi^2 \gamma_m^2 \mathfrak{F}} \int_0^{x_P} \frac{x^3 \exp(x) dx}{[\exp(x) - 1]^2 \tan^{-1}(Ax)}, \quad (\text{A1})$$

where  $M = w/(Ls)$  is the mass of a unit cell with  $L$  designating Avogadro's number. We obtain an intermediate temperature limit if  $T$  is sufficiently large that the above approximations are valid, but not so large that  $Ax$  is small over the contributing region of  $x$ . In this circumstance,  $\tan^{-1}(Ax) \approx \pi/2$ , and the conventional  $T^{-1}$  high-temperature limit follows. If also the acoustic modes are assumed to be nondispersive so that  $g = b = \bar{n}^{1/3}$ , and we consider only the simplest lattices with optic modes,  $\bar{n} = 2$ , Eq. (A1) yields, with  $a \equiv \pi^{-1/3}$ ,

$$K \approx 0.04138 (k_B/\hbar)^2 M a T_D^3 / (\pi^3 \gamma_m^2 T). \quad (\text{A2})$$

This result is similar to that of Roufosse and Klemens<sup>33</sup> who obtained 0.03491 for the numerical coefficient. For a lattice with  $\bar{n} = 1$  (no optic modes), the two-fluid model requires a region of dispersive acoustic modes to produce a finite value of  $K$ . If the fraction  $f_A$  of flat acoustic modes as used in the text [cf. Eq. (38)] is employed to describe these, we may take, e.g.,  $\omega_p = \omega_D = (6\pi^2)^{1/3} c_m/a$  for the maximum frequency of a nondispersive longitudinal mode, and a frequency  $\omega_{RU} = (6\pi^2)^{1/3} c_m/(2^{1/3}a)$  near the Debye zone boundary (Ref. 3, Sec. 1.11) as the point where the transverse modes become dispersive (viz., for  $\omega < \omega_{RU}$  we take them as nondispersive, with a plateau at  $\omega = \omega_{RU}$ ). For these values,  $g = 1$ ,  $\mathfrak{F} = \frac{1}{3}$ , we obtain

$$K = 0.2566 (k_B/\hbar)^3 M a T_D^3 / (\pi^3 \gamma_m^2 T).$$

This coefficient is close to the result  $3(4)^{1/3}/20$

$= 0.2381$  of Liebfried and Schlömann<sup>13</sup> and corrected by Julian.<sup>33</sup> Smaller values of  $\omega_{RU}$  corresponding to a larger region of dispersive modes decreases  $K$  (by increasing  $\mathfrak{F}$ ) relative to the Liebfried-Schlömann magnitude toward the Roufosse-Klemens result. Thus, as would be expected, the coefficient depends sensitively upon the amount of dispersion present in the acoustic modes and/or the presence of optic modes.

## 2. Very-high-temperature limit

At still higher temperatures, the reservoir relaxation time is expected to become small, possibly approaching a minimum value.<sup>7</sup> Because propagation frequencies cannot exceed the frequency of the highest nondispersive modes of the lattice,  $\omega_p \bar{\tau}$  may ultimately become small (since  $\bar{\tau} \propto T^{-1}$ ) such that we can set  $\tan^{-1} 2\omega \bar{\tau} \approx 2\omega \bar{\tau}$  in Eq. (17) of the text. [The WE theory rather than LR theory justifies Eq. (17) in this limit; however, we assume that the temperature and velocity shifts defined by WE will vanish for such very high-frequency waves. It would not be meaningful to define temperature and velocity differences over the scale of a few lattice spacings.] Thus, the "very-high-temperature" limit of Eq. (A1) is

$$K \approx \frac{M c_m \omega_p}{6\pi^2 \gamma_m^2 \langle \tau \rangle_{av} \mathfrak{F} T} \quad (\text{A3})$$

where  $\langle \tau \rangle_{av}$  signifies an average over the reservoir specific-heat factor  $C_{\omega_j}^{(w)}$  as defined in Eq. (36) of Ref. 31.

We use the high-temperature U-process  $\tau$  of Roufosse and Klemens,<sup>33</sup>

$$\tau = \sqrt{2} M c^3 / (4\pi \gamma^2 a k_B T \omega^2), \quad (\text{A4})$$

and estimate  $\langle \omega^{-2} \rangle_{av}$  in the Debye approximation.<sup>10</sup> Estimating  $\omega_{RC}$  as  $1.3\omega_D$ , setting  $\omega_p = \omega_D/g = \omega_D/\bar{n}^{1/3}$ , and assuming  $\gamma$  and  $c$  of Roufosse and Klemens are the same as our  $\gamma_m$  and  $c_m$ , we obtain from Eq. (A3)

$$K \approx 3.1 \pi a c_m \rho s \bar{n}^{2/3} R / (w \mathfrak{F}), \quad (\text{A5})$$

a result that is independent of temperature. Slack<sup>7</sup> has discussed this very-high-temperature leveling off of  $K$  and derived a similar limit that agrees with the scanty experimental data available. Using Slack's data (Table XVIII of Ref. 7) for the material constants of these crystals, and the estimate  $\mathfrak{F} \approx 2.5$  ( $\bar{n} = 3$ ), Eq. (A5) yields  $K \approx 29$  mW/cm deg for  $\text{ZrO}_2$  and 25 mW/cm deg for  $\text{ThO}_2$ , in reasonable agreement with the experimental data cited by Slack. It should be noted that no artificial assumption has been made regarding the mean free path of either the optic or acoustic phonons in the above derivation.

## APPENDIX B: LOW-TEMPERATURE N- AND U-PROCESS RELAXATION TIMES

### 1. N-process relaxation time

The low-temperature reservoir theory presented in Sec. IIC of the text can be compared to conventional results for the Callaway N-process relaxation time. The parameter usually quoted is  $\langle \tau_N^{-1}(x) \rangle_{av}$  where the angular bracket  $\langle \rangle_{av}$  is the specific-heat-weighted modal average as defined in Appendix A. Performing this average on  $\tau_{ANR}^{-1}(x)$  of Eq. (27) of the text yields

$$\langle \tau_{ANR}^{-1}(x) \rangle_{av} = 5QH(x_R)T^5\zeta(5)/\zeta(4) = 4.7903QH(x_R)T^5. \quad (B1)$$

If the low-temperature reservoir boundary in the  $\nu$ - $T$  plane is approximated as a straight line,  $H(x_R)$  is independent of  $T$ , and Eq. (B1) has the form obtained in some previous studies of LiF, NaF, and solid  $^3\text{He}$ - $^4\text{He}$  mixtures.<sup>27-32</sup> The only free parameter here is the reservoir boundary slope  $x_R$ , so it is of interest to calculate the value of  $x_R$  that produces numerical agreement with  $\langle \tau_N^{-1} \rangle_{av}$  of previous studies.

From an analysis of Thacher's LiF thermal-conductivity data,<sup>23</sup> Guyer and Sarkissian<sup>27</sup> obtained  $\langle \tau_N^{-1} \rangle_{av} = 0.5T^5 \text{ sec}^{-1}$ . This corresponds to  $H(x_R) = 0.6$  and  $x_R \approx 10.3$  in Eq. (B1) with  $Q = 0.16 \text{ sec}^{-1} \text{ deg}^{-5}$  as used earlier, in qualitative agreement with curve (b) of Fig. 2 of the text.

Numerical computations of  $H(x_R)$  were performed for LiF to assess the error of the straight-line approximation to  $x_R$ . For Thacher's curve B (Fig. 4 of Ref. 23) with  $\alpha = 0.126 \text{ sec}^{-1} \text{ deg}^{-4}$  for isotope scattering, it was found that  $H(x_R)$  varied approximately as  $T^{-1/2}$  for  $T$  between 10 and 100 K. Thus,  $\langle \tau_{ANR}^{-1} \rangle$  actually goes as  $T^{4.5}$  rather than  $T^5$ . This may account for the finding by Berman and Brock<sup>17</sup> and Rogers<sup>45</sup> that they could fit their data with  $\langle \tau_N^{-1} \rangle \propto T^4$  rather than the more canonical  $T^5$  form.

### 2. Apparent U-process relaxation time

It is of interest to reconcile the lack of a separate U-process transition rate in the two-fluid theory with the conventional approach. By definition, the high-temperature reservoir lies above a constant angular frequency  $\omega_{RU}$ . Thus, it turns out that use of  $\omega_{RU} = \omega_D/b$  as the lower limit of integration for the specific heat  $\Delta C_R^{(w)}$  causes this quan-

tity to exhibit the behavior of the conventional U-process factor  $\exp[-T_D/(bT)]$  in the appropriate temperature range. The anharmonic transition rate  $\tau_{ANR}^{-1}$ , given by Eq. (19) of the text, is proportional to  $\Delta C_R^{(w)}$  so it, in turn, exhibits this same behavior. To show this, we use the Debye approximation to compute  $\Delta C_R^{(w)}$  because this approximation was used in the analyses with which we compare. Thus, Eqs. (26)–(29) of the text provide  $\Delta C_R^{(w)}$  and  $\tau_{ANR}^{-1}$  in terms of the complementary Debye function  $H(x_{RU})$ . Its asymptotic expansion,<sup>22</sup> valid for  $x_{RU} \equiv \hbar\omega_{RU}/(k_B T)$  somewhat greater than unity, is

$$H(x_{RU}) \approx \exp(-x_{RU})(x_{RU}^4 + 4x_{RU}^3 + 12x_{RU}^2 + 24x_{RU} + 24), \quad (B2)$$

where only the first term in powers of  $\exp(-x_{RU})$  has been retained. Thacher<sup>23</sup> fitted his data with  $T_D/b = 186 \text{ K}$ , and the value used by Berman and Brock<sup>17</sup> was similar. Thus, we set  $x_R = 186/T$ , again use  $Q = 0.16 \text{ sec}^{-1} \text{ deg}^{-5}$  and obtain

$$\tau_{ANR}^{-1}(x) = x \exp(-186/T)(6.6 \times 10^4 T^3 + 714 T^4 + \dots), \quad (B3)$$

where only terms in  $T^3$  and  $T^4$  are explicitly displayed since these correspond to the temperature dependence of the U-process terms used in Refs. 17 and 23. The first term of Eq. (B3) is similar to Thacher's term  $5.3 \times 10^4 x^2 T^3 \exp[-186/T]$ , and the second is similar to that of Berman and Brock, which was  $600x^2 T^4 \exp[-170/T]$ . The  $x^2$  dependence of their expressions is not well established or unique; other authors have used the  $x$  dependence of Eq. (B3).<sup>1,32</sup> Thus,  $\tau_{ANR}^{-1}$  contains terms that behave like conventional U-process rates. In the example above, the last term of Eq. (B2) becomes important for temperatures above 100 K, where it causes  $\tau_{ANR}^{-1}$  to decrease less rapidly with  $T$  than a single-term expression such as used in Ref. 17. This explains why the two-fluid expression continues to represent  $K$  towards higher temperatures better than, e.g., the Berman-Brock fit. Towards low  $T$ , the extrinsic reservoir causes the lower limit of integration of  $\Delta C_R^{(w)}$  to drop in such a way that the exponential behavior shown above ceases, and is replaced by the behavior conventionally associated with the N-process rate. In other words,  $\tau_{ANR}^{-1}$  becomes the N-process rate in the low-temperature limit and contains the conventional U-process rate, in addition to other terms, in the high-temperature limit.

\*Part of this work was carried out while the author was on temporary assignment to the Department of Aeronautics and Astronautics, Stanford University, Stan-

ford, CA 94305.

<sup>1</sup>P. G. Klemens, in *Solid-State Physics*, edited by F. Seitz and D. Turnbull (Academic, New York, 1958),

- Vol. 7, p. 1.
- <sup>2</sup>P. G. Klemens, in *Thermal Conductivity*, edited by R. P. Tye (Academic, London, 1969), Vol. 1, p. 1.
  - <sup>3</sup>J. M. Ziman, *Electrons and Phonons* (Oxford University Press, London, 1963).
  - <sup>4</sup>P. Carruthers, *Rev. Mod. Phys.* **33**, 92 (1961).
  - <sup>5</sup>J. E. Parrott and Audrey D. Stuckes, *Thermal Conductivity of Solids* (Pion, London, 1975).
  - <sup>6</sup>R. Berman, *Thermal Conduction in Solids* (Oxford University Press, London, 1976).
  - <sup>7</sup>Glen A. Slack, in *Solid-State Physics*, edited by Henry Ehrenreich, Frederick Seitz, and David Turnbull (Academic, New York, 1979), Vol. 34.
  - <sup>8</sup>T. O. Woodruff and H. Ehrenreich, *Phys. Rev.* **123**, 1553 (1961).
  - <sup>9</sup>Humphrey J. Maris, in *Physical Acoustics*, edited by W. P. Mason and R. N. Thurston (Academic, New York, 1971), Vol. VIII, p. 279.
  - <sup>10</sup>B. H. Armstrong IBM Palo Alto Scientific Center Report No. G320-3408, 1980 (unpublished).
  - <sup>11</sup>N. F. Mott and H. Jones, *The Theory of the Properties of Metals and Alloys* (Dover, New York, 1958), p. 265.
  - <sup>12</sup>Joseph Callaway, *Phys. Rev.* **113**, 1046 (1959).
  - <sup>13</sup>Günther Liebfried and Ernst Schlömann, *Nachr. Akad. Wiss. Goettingen Math. Phys. Kl. 2A Math. Phys. Chem. Abt. IIa*, 71 (1954).
  - <sup>14</sup>Transitions for which  $\vec{q}'$  is in region 1 and  $\vec{q}''$  in region 2 are ignored. This is based on the tendency for  $\vec{q} + \vec{q}' \rightarrow \vec{q}''$  absorption to be dominated by processes for which  $|\vec{q}'| \approx |\vec{q}''| \gg |\vec{q}|$ . The ultimate choice of reservoir boundary will be adjusted so that neglected transitions can implicitly influence the result.
  - <sup>15</sup>Eugene I. Blount, *Phys. Rev.* **114**, 418 (1959).
  - <sup>16</sup>P. G. Klemens, *Proc. R. Soc. London* **A208**, 108 (1951).
  - <sup>17</sup>R. Berman and J. C. F. Brock, *Proc. R. Soc. London* **A289**, 46 (1965).
  - <sup>18</sup>Isotope scattering actually goes as  $\tau^{-1} \propto \omega^2 dN/d\omega$ , where  $dN/d\omega$  is the density of states (Ref. 4). Departure of  $dN/d\omega$  from the Debye approximation should be significant only above our U-process reservoir threshold since this is where significant dispersion appears. We can neglect this effect because the  $\omega^4$  Rayleigh scattering form will only be used to determine the reservoir threshold for frequencies below the U-process reservoir threshold. This is especially convenient to permit the combination of effects of impurities and isotopes in a simple manner.
  - <sup>19</sup>To render the omission of  $\tau_{\text{ANN}}^{-1}$  from these inequalities more perspicuous, think of the scattering in transition metals. The two-band model is important when  $s$ - $d$  transitions dominate the resistive processes within the  $s$  band. Such a condition is equivalent to the relations (23)-(24).
  - <sup>20</sup>Peter Carruthers, *Phys. Rev.* **126**, 1448 (1962).
  - <sup>21</sup>Charles Kittel, *Introduction to Solid State Physics*, 4th ed. (Wiley, New York, 1971).
  - <sup>22</sup>M. Abramowitz and I. A. Stegun, editors, *Handbook of Mathematical Functions* (National Bureau of Standards, Washington, D. C., 1964).
  - <sup>23</sup>Philip D. Thacher, *Phys. Rev.* **156**, 975 (1967).
  - <sup>24</sup>K. O. McLean and C. S. Smith, *J. Phys. Chem. Solids* **33**, 279 (1972).
  - <sup>25</sup>O. L. Anderson, in *Physical Acoustics*, edited by Warren P. Mason (Academic, New York, 1965) Vol. IIB, p. 43.
  - <sup>26</sup>G. Dolling, H. G. Smith, R. M. Nicklow, P. R. Vijayaraghavan, and M. K. Wilkinson, *Phys. Rev.* **168**, 970 (1968).
  - <sup>27</sup>C. C. Ackermann and R. A. Guyer, *Ann. Phys. (N. Y.)* **50**, 128 (1968).
  - <sup>28</sup>E. M. Hogan, R. A. Guyer, and H. A. Fairbank, *Phys. Rev.* **185**, 356 (1969).
  - <sup>29</sup>Joseph Callaway, *Phys. Rev.* **122**, 787 (1961).
  - <sup>30</sup>Bal Krishna Agrawal, *Phys. Rev.* **162**, 731 (1967).
  - <sup>31</sup>Howard E. Jackson and Charles T. Walker, *Phys. Rev. B* **3**, 1428 (1971).
  - <sup>32</sup>M. G. Holland, *Phys. Rev.* **132**, 2461 (1963).
  - <sup>33</sup>Micheline Roufosse and P. G. Klemens, *Phys. Rev. B* **7**, 5379 (1973).
  - <sup>34</sup>Lawrence A. Vredevoe, *Phys. Rev.* **140**, A930 (1965).
  - <sup>35</sup>P. G. Klemens, *J. Appl. Phys.* **38**, 4573 (1967).
  - <sup>36</sup>G. Nilsson and G. Nelin, *Phys. Rev. B* **3**, 364 (1971).
  - <sup>37</sup>R. Berman, C. R. Day, D. P. Goulder, and J. E. Vos, *J. Phys. C* **6**, 2119 (1973).
  - <sup>38</sup>R. H. Crepeau, O. Heybey, D. M. Lee, and Stanley A. Strauss, *Phys. Rev. A* **3**, 1162 (1971).
  - <sup>39</sup>Private communication.
  - <sup>40</sup>Y. S. Touloukian, R. W. Powell, C. Y. Ho, and P. G. Klemens, *Thermal Conductivity—Non-metallic Solids*, Vol. 2 of *Thermophysical Properties of Matter, The TPRC Data Series* (IFI Plenum, New York, 1979).
  - <sup>41</sup>V. J. Minkiewicz, T. A. Kitchens, F. P. Lipschultz, R. Nathans, and G. Shirane, *Phys. Rev.* **174**, 267 (1968).
  - <sup>42</sup>R. A. Reese, S. K. Sinha, T. O. Brun, and C. R. Tilford, *Phys. Rev. A* **3**, 1688 (1971).
  - <sup>43</sup>H. Bialas, O. Weis, and H. Wendel, *Phys. Lett.* **43A**, 97 (1973).
  - <sup>44</sup>J. G. Traylor, H. G. Smith, R. M. Nicklow, and M. K. Wilkinson, *Phys. Rev. B* **3**, 3457 (1971).
  - <sup>45</sup>J. Rogers, *Phys. Rev. B* **3**, 1440 (1971).